# Demonstration of an In-Building Optical Bus Network for Wireless Access

Yannis Le Guennec, Zine Bouhamri, Jean-Marc Duchamp, Béatrice Cabon

# Demonstration of In-Building Optical Bus Network For Wireless Access

Yannis Le Guennec, Zine Bouhamri, Jean-Marc Duchamp and Béatrice Cabon

***Abstract*— This paper presents the demonstration of a distributed antenna system (DAS) based on a radio-over-fiber (RoF) bus for wireless local area networks (WLAN). RoF bus has been designed based on the use of cascaded building blocks to support a large number of access nodes using electronic coupling and in-line amplification inside the access nodes. A dedicated emulation protocol has been defined to test the RoF bus and experimental results have shown that a coverage distance of about 4.5 meters is obtained for bi-directional communications up to 18 access nodes. For large buildings, a star-bus network, based on multiple interconnected RoF buses is proposed, and significant reduction of in-building deployed fiber length is achieved (89%) compared to a RoF star network infrastructure.**

***Index Terms*— optical bus; radio-over-fiber; distributed antenna system; VCSEL; WLAN; multimode fiber.**

## I. Introduction

The next generation of in-building wireless access networks will require a significant increase of the capacity and a reduced power consumption for "Green" networking [1] and for extending the autonomy of battery-powered devices, with a limited overall electromagnetic radiation exposure for the user [2]. However, in nowadays in-building wireless local area networks (WLAN), severe radio propagation conditions leads to under optimum connexion data rates while wireless transmitters deliver maximum radio power authorized by telecommunication regulations, limiting the autonomy of battery powered devices.

A straightforward solution to address the aforementioned issues is to reduce the size of deployed radio cells, which results in a weaker impact of the radio channel on the transmitted radio signal and also in the possibility of decreasing the emitted power by the radio transmitter antenna. However, the deployment of small radio cells (femtocells) requires the set-up of a large number of access points to cover an equivalent area, which may increase drastically the network cost and complexity, since "networking intelligence" is embedded in each access point [3]. Fiber-fed distributed antenna systems (DAS) have attracted much attention [4]-[6]. Indeed, a large number of access nodes (AN), without intelligence, can be fed with optical fibers which exhibit low loss, large bandwidth and immunity to interference. Due to its large bandwidth, optical fiber offers the possibility to deliver multiple narrowband radio standards [7] or ultra wideband radio (UWB) [8] to the users. These radio-over-fiber (RoF) DAS support either analog or digitized radio. Digitized RoF allows lifting the constraint of highly linear electrical/optical transceivers necessary in analog RoF DAS, but requires additional wide bandwidth digital to analog converters with sufficient resolution in the numerous ANs [9].

RoF DAS uses preferably intensity modulation and direct detection (IMDD) and multimode fibers (MMF) to decrease the overall cost of the system. Design of IMDD DAS has been extensively studied, particularly for point to point (P2P) systems in star network topology [10]-[11], and it has been shown that RoF DAS provides better throughput and energy efficiency than typical centralized radio deployment [12]-[14]. Nevertheless, star network topology introduces several disadvantages, such as the large duct diameter and the increased cost of array optical transceivers. Regarding installation costs, point-to-multipoint (P2MP) topologies is recommended because of a larger sharing factor of the fiber cables and smaller duct diameters leading to a reduced capital expenditure (CapEx) [15].

Recently, UWB RoF bus over large core plastic optical fibers (POF) has been demonstrated to reduce the CapEx for in-building networks [16]. Optical distribution of UWB signal to the different ANs is realised by the use of cascaded optical power splitters to feed the different ANs. Nevertheless, since optical power is shared between the different ANs and strongly attenuated by the POF sections, UWB signal to noise ratio is significantly impacted after transmission to the 3rd AN. To compensate for the optical loss, large optical power laser source can be used at the RoF bus input, but in-building optical network deployment will probably require limited optical power transmission for safety purpose.

In [17], we have proposed a RoF bus using electronic coupling to feed the AN RF front-end, and electronic in-line amplification to compensate for electronic coupler loss, so the number of ANs in the bus can be extended. Each building block of the RoF bus uses 2 similar optical links (one for down-link, one for up-link), with laser sources exhibiting a limited optical power of around 1 mW. We have shown theoretically in [17] that, although the cascade of several optical links in the RoF bus infrastructure induces a significant increase of the bus noise figure, we could expect around 20 ANs to be fed with the RoF bus infrastructure, including the possibility of multistandard radio compatibility. However, a careful design of the RoF bus is required.

In this article, for the first time, an experimental demonstration of a RoF bus over MMF, using electronic coupling in the AN, is provided for in-building WLAN network. In Section II, RoF bus principle is presented based on

the concept of *N* cascaded building blocks, and RoF bus down-link and up-link design rules are described. Based on these design rules, a RoF bus prototype has been specified in Section III. The system has been tested using a dedicated experimental protocol based on signal emulation exposed in Section IV, and experimental results are discussed for down-link and up-link. Discussion for practical deployment of the proposed RoF bus is provided in Section V together with estimation of the necessary fiber length to deploy in comparison with RoF star architecture.

## II. RoF Bus System

### A. RoF bus building blocks

As seen on Fig. 1, a building block of the RoF bus is composed of 2 optical links (one for the down-link, another for the up-link) and one AN. A building block is defined as an elementary element to be cascaded in order to realise the RoF bus infrastructure. The input of first building block is connected to the central station which is typically a WLAN access point with centralized network intelligence. For the RoF bus down-link (Fig. 1a), the WLAN signal is transmitted over an optical link, made of a laser source, an optical fiber and a photodetector. The output electrical signal of the optical link is amplified using an in-line amplifier before being sent to a coupler *x/1-x* allowing for the separation of signal power. Some power can be directed towards the RF front-end, the other part being sent to the following building block #*n*+1.

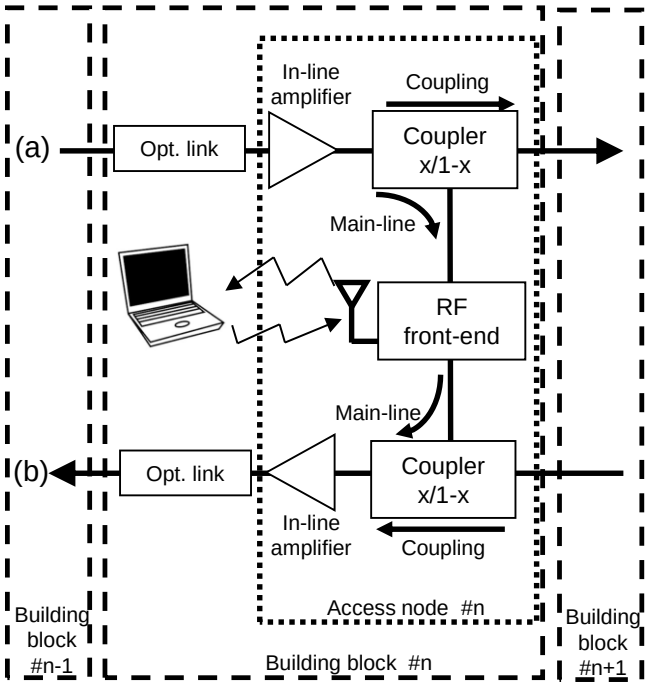


Figure 1. RoF bus infrastructure (a) downlink (b) up-link. Opt. link: optical link.

For the RoF bus up-link (Fig. 1b), the received radio signal by the RF front-end is send into a coupler *x/1-x* to be combined with coupled up-link signal from building block #*n*+1. Both signals are amplified with an in-line amplifier. At the amplifier output, the signal is transmitted through the optical link to reach building block #*n*-1, and the following, to be finally received by the central station.

Since a building block is defined as an elementary element of the RoF bus, gain transparency must be achieved for the transmission over one building block for both down-link and up-link. To meet this requirement, the gain of the optical links ($G_{opt}$) has been defined as:

$$G_{opt} = 1 \tag{1}$$

The gain of the in-line amplifier ($G_{in\text{-}line}$) used for down-link and up-link is defined to compensate for the main-line gain ($G_{coup(x)}$) of the coupler *x/1-x* (Fig. 1) as:

$$G_{in-line} = \frac{1}{G_{coup(x)}} \tag{2}$$

### B. RoF bus compression point and operating conditions

The non-linear behavior of the RoF bus is a critical specification because it may impact on signal integrity. The optical bus 1-dB input compression can be expressed from 1-dB compression points and gains of all cascaded elements [18]. For the downlink (Fig. 1a), the overall 1-dB compression point ($CP_{DL}$) can be expressed as:

$$\frac{1}{CP_{DL}} = \sum_{i=1}^{N} \frac{G_{opt}^{i-1} G_{coup(x)}^{i-1} G_{in-line}^{i-1}}{CP_{opt}} + \sum_{i=1}^{N} \frac{G_{opt}^{i} G_{coup(x)}^{i-1} G_{in-line}^{i-1}}{CP_{in-line}} + \sum_{i=1}^{N} \frac{G_{opt}^{i} G_{coup(x)}^{i-1} G_{in-line}^{i}}{CP_{coup(x)}} + \frac{G_{coup(1-x)} G_{opt}^{N} G_{coup(x)}^{N-1} G_{in-line}^{N}}{CP_{RF\ DL}} \tag{3}$$

where *N* is the number of cascaded building blocks, $CP_{opt}$, $CP_{in\text{-}line}$ , $CP_{coup(x)}$ and $CP_{RF\ DL}$ are the 1-dB compression points of the optical link, in-line amplifier, *x/1-x* coupler and RF front-end down-link respectively, $G_{coup(1-x)}$ is the coupler coupling gain, $G_{RF\ DL}$ is the gain of the down-link RF front-end. Considering the gain transparency conditions for the optical bus ((1) and (2)), and that *x/1-x* coupler is a linear device, (3) can be simplified as:

$$\frac{1}{CP_{DL}} = \frac{N}{CP_{opt}} + \frac{N}{CP_{in-line}} + \frac{G_{coup(1-x)} G_{in-line}}{CP_{RF\ DL}} \tag{4}$$

The in-line amplifier can be specified to exhibit $CP_{in\text{-}line} >> CP_{opt}$ and $CP_{RF\ DL}$ can be specified to make it negligible the last term of the sum in (4) with respect to the first term, leading to:

$$CP_{DL} \approx \frac{CP_{opt}}{N} \tag{5}$$

The same approach is used to evaluate the 1-dB compression point for the RoF bus up-link ($CP_{UL}$):

$$CP_{UL} \approx \frac{CP_{opt}}{N G_{RF\ UL} G_{coup(1-x)} G_{in-line}} \tag{6}$$

where $G_{RF\ UL}$ is the up-link RF front-end gain.

The down-link and up-link must be operated with a WLAN modulation power ($P_{MOD\ DL}$ and $P_{MOD\ UL}$ respectively) exhibiting a power back-off from the RoF bus 1-dB input

compression point, to avoid a significant impact of the non-linearity on the radio signal. This power back-off corresponds to the WLAN peak to average power ratio (PAPR) [19]:

$$P_{MOD\ DL/UL} = \frac{CP_{DL/UL}}{PAPR} \tag{7}$$

### C. Down-link specifications

Down-link (Fig. 1a) is defined as $N$ cascaded building blocks except that the output of the $N^{th}$ building block is the RF-front-end output. Considering (1) and (2), the down-link gain ($G_{DL}$) can be defined as:

$$G_{DL} = G_{in-line} G_{coup(1-x)} G_{RF\ DL} \tag{8}$$

Optical link noise figure ($NF_{opt}$) and $G_{opt}$ are assumed to be independent of fiber length in the range up to 100 m, which is supposed to be the maximum fiber length between 2 ANs in the RoF bus network topology. $NF_{opt}$ has been found to be several orders of magnitude greater than the other bus elements' noise figure. It has been found in [17] that the noise figure for the RoF bus down-link ($NF_{DL}$), can be approximated as:

$$NF_{DL} \approx N\ NF_{opt} \tag{9}$$

As seen from (9), the cascade of $N$ building blocks induces an increase of the overall bus noise figure noise, leading to a decrease of the signal to noise ratio (SNR) at the AN RF front-end output. The error vector magnitude (EVM) at the AN RF front-end output can be derived from (9) [20]:

$$EVM = \sqrt{\frac{NF_{DL}}{SNR_{in}}} \tag{10}$$

where $SNR_{in}$ is the input SNR of the RoF bus. Since the EVM for the WLAN transmitter is limited by the IEEE 802.11g standard, the maximum number of building blocks will be limited as well.

Concerning the WLAN receiver, WLAN sensitivity ($S_{WLAN}$) is defined as:

$$S_{WLAN} = NF_{WLAN}\, SNR_{req}\, kT_0\, B \tag{11}$$

where $SNR_{req}$ is the required signal to noise ratio at the WLAN receiver output to satisfy a BER of $10^{-5}$, $NF_{WLAN}$ is the WLAN receiver noise figure, $k$ is the Boltzmann constant, $T_0$ is the ambient temperature of 298 K, $B$ is the WLAN signal bandwidth.

Maximum radio propagation path loss ($PL$) is derived from (11):

$$PL = \frac{P_{TX}\, G_{ANT}\, G_{ANT\ MU}}{S_{WLAN}} \tag{12}$$

where $P_{TX}$ is the transmitted power fed into the RF front-end down-link antenna derived from (7) and (8), $G_{ANT}$ is the AN antenna gain, $G_{ANT\ MU}$ is the mobile unit antenna gain. Down-link radio coverage can be evaluated from (12), considering a free space radio propagation model, one AN being deployed per building room with light of sight (LOS) transmission [21].

### D. Up-link specifications

Up-link (Fig. 1b) is defined as $N$ cascaded building blocks, the input of the first building block being the RF front-end input. The gain for the up-link, considering (1) and (2), is defined as:

$$G_{UL} = G_{in-line} G_{coup\,(1-x)} G_{RF\ UL} \tag{13}$$

Up-link noise figure ($NF_{UL}$) is expressed as:

$$NF_{UL} \approx \frac{N\ NF_{opt}}{G_{UL}} \tag{14}$$

Up-link sensitivity ($S_{UL}$) is defined as the minimum power to receive at the $N^{th}$ access node RF front-end antenna input to reach $SNR_{req}$ at the central station and is expressed as:

$$S_{UL} = NF_{UL} SNR_{req}\, kT_0\, B \tag{15}$$

### E. Radio coverage

Considering a bi-directional WLAN transmission, with equal transmitter power $P_{TX}$ for the AN and mobile unit, similar $PL$ (i.e radio coverage) for down-link and up-link is achieved when the sensitivity of the RoF bus up-link ($S_{UL}$) (15) equals to $S_{WLAN}$ (11) leading to the following condition:

$$NF_{UL} = NF_{WLAN} \tag{16}$$

From (13), (14) and (16), one can derive a condition for the up-link RF front-end gain to provide bidirectional communication capability:

$$G_{RF\ UL} = \frac{N\ NF_{opt}}{NF_{WLAN}\, G_{coup(1-x)}\, G_{in-line}} \tag{17}$$

The RF front-end up-link amplifier gain (17), together with the gain of the in-line amplifier (2), compensate for the increase of $NF_{UL}$ with the number of cascaded optical links (14).

## III. PROTOTYPE

### A. Point-to-point Optical Link Specifications

Optical links have been designed and tested to be used in building blocks defined in Section II. These optical links use components off-the-shelf (COTS) for a low-cost approach. Two MMF optical links have been designed. One is based on the use of a VCSEL, emitting at wavelength 850 nm, and p-i-n photodiode with a built-in transimpedance amplifier (TIA), the other one is based on the use of a transmitter optical subassembly (TOSA), emitting at wavelength 1300 nm, and a receiver optical subassembly (ROSA) from Finisar. The former has been already used for radio transmission over fiber, exhibiting high linearity [8], the latter is dedicated to 10 Gbps Ethernet. For both systems, 100 m length OM2 MMF with 50/125 µm core/cladding diameters is used. Measured $G_{opt}$, $NF_{opt}$ and $CP_{opt}$ are reported in Tab. I. Both optical links have been designed to achieve gain transparency (1).

TABLE I
OPTICAL LINKS SPECIFICATIONS

| | VCSEL/PIN | TOSA/ROSA |
|---|---|---|
| $G_{opt}$ (dB) | 0 | 0 |
| $NF_{opt}$ (dB) | 39 | 45 |
| $CP_{opt}$(dBm) | 0 | -17 |

TABLE II
RADIO SPECIFICATIONS FOR WLAN 802.11G

| | | |
|---|---|---|
| | Modulation technique | 64-QAM OFDM |
| $B$ | WLAN bandwidth | 16.6 MHz |
| $D$ | WLAN data rate | 54 Mbps |
| $PAPR$ | WLAN peak to average power ratio at probability 1m% | 12 dB |
| $EVM_{req}$ | Required EVM at WLAN transmitter output | -25 dB |
| $SNR_{req}$ | Required signal to noise ratio at WLAN receiver output | -18.5 dBm |
| $NF_{WLAN}$ | WLAN receiver noise figure | 8 dB |
| $S_{WLAN}$ | WLAN receiver Sensitivity | -75.3 dBm |

### B. *Transmission of WLAN over One Optical Link*

WLAN IEEE 802.11g, based on orthogonal frequency division multiplexing (OFDM) at carrier frequency 2.4 GHz, is generated from a vector signal generator Agilent ESG4438C and directly modulates the laser source (VCSEL or TOSA). Output optical link radio signals are analyzed with Agilent 89611 VXI-based Analyzer and 89600 Vector Signal Analysis software. WLAN IEEE 802.11g standard specifications are reported in Tab. II. EVM is measured at VCSEL/PIN and TOSA/ROSA optical links output and reported in Fig. 2. Fig. 2 shows that, for low WLAN modulation power, EVM is impacted by optical link noise (mainly due to photodetected laser relative intensity noise (RIN) [8]). For high modulation power, EVM of WLAN increases significantly due optical link non-linearity [22]. From Fig. 2, it can be seen also that TOSA/ROSA optical link exhibits stronger non-linear impact on EVM than VCSEL/PIN link due to its lower 1-dB compression point (Tab. I). As predicted by (7), considering $N$=1, the WLAN modulation power for which EVM is minimized (i.e -12 dBm and -29 dBm for VCSEL/PIN and TOSA/ROSA respectively) corresponds to the 1-dB input compression point with a back-off corresponding to the WLAN PAPR.

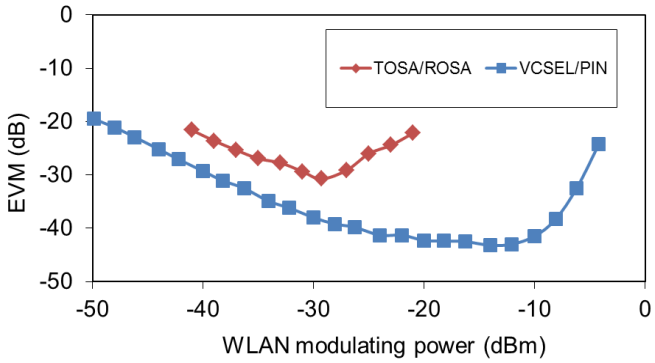


Figure 2. Measured EVM as a function of WLAN modulating power for VCSEL/PIN and TOSA/ROSA optical links

### C. *RoF bus and Access Node Specifications*

With a target of $N=20$ cascaded building blocks for the optical bus, laser source modulation power has been defined at $P_{MOD\ DL}$=-25 dBm for VCSEL PIN and $P_{MOD\ DL}$=-42 dBm for TOSA/ROSA taking into account the reduced 1-dB compression point for the RoF bus (7). From (8), downlink radio transmitted power at AN output is found to be $P_{TX\ DL}$=-20.5 dBm for VCSEL/PIN based RoF bus and $P_{TX\ DL}$=-36.5 dBm for TOSA/ROSA based RoF bus. In case of LOS free space propagation, the expected radio coverage derived from (12) is around 11 m for VCSEL/PIN based RoF bus, but it is reduced to around 2 m for TOSA/ROSA based RoF bus.

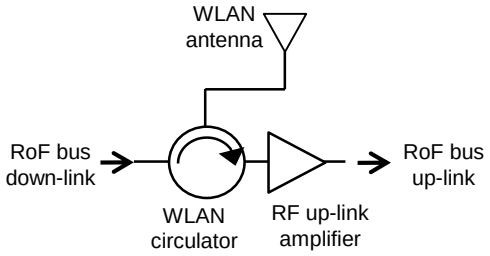


Figure 3. Access node RF front-end.

The AN RF front-end design is shown in Fig. 3. A WLAN circulator is used to separate up-link and down-link radio, WLAN operating in half-duplex mode. Tab. III summarizes the specifications for the AN and mobile unit RF components, following the RoF bus design rules exposed in Section II. A large gain for the up-link RF front-end ($G_{RF\ UL}$ =34.5 dB) is needed to compensate for the increase of $NF_{UL}$ (14)with the number of cascaded building blocks $N$.

TABLE III
ACCESS NODE AND MOBILE UNITS SPECIFICATIONS

| | | |
|---|---|---|
| $G_{IN\text{-}LINE}$ | In-line amplifier gain | 10 dB |
| $G_{COUP(1\text{-}x)}$ | Coupler main-line gain | -0.5 dB |
| $G_{COUP(x)}$ | Coupler coupling gain | -10 dB |
| $G_{RF\ DL}$ | RF front-end gain for down-link | -5 dB |
| $G_{RF\ UL}$ | up-link RF front-end gain | 34.5 dB |
| $G_{ANT}$ | Access node antenna gain | 3 dB |
| $G_{ANT\ MU}$ | Mobile unit antenna gain | 3 dB |

## IV. EXPERIMENTAL PROTOCOL AND RESULTS

### A. *Experimental Protocol for RoF bus Testing*

Due to the possible large number of cascaded building blocks in the RoF bus architecture ($N$=20), we have developed a dedicated experimental protocol to test the RoF bus. A physical transmission of WLAN has been realized over a single building block (Fig. 1). The output signal of the building block has been captured with the vector signal analyser recorder and playback physically with the arbitrary waveform generator (AWG) included in the vector signal generator and fed into the same building block to emulate the transmission over 2 cascaded building blocks, as shown on Fig. 4. The process is repeated for the transmission over $N$ blocks of the RoF bus.

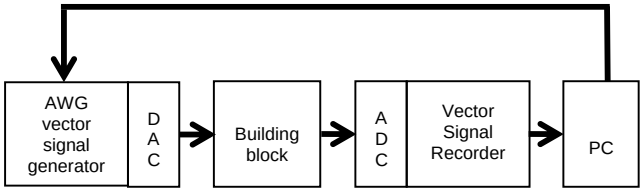


Figure 4. Test bench for RoF bus infrastructure using emulation protocol. DAC: Digital to Analog Conversion. ADC: Analog to Digital Conversion

### B. *Validation of the Experimental Protocol*

To validate the emulation protocol described in Section IV.A, 3 building blocks based on TOSA/ROSA optical link have been realized matching specifications from Tab. I. Measured EVMs after real transmissions over the 3 building blocks have been compared to the measured EVM using the emulation protocol. Results are reported in Tab. IV.

TABLE IV
EMULATION PROTOCOL VALIDATION WITH TOSA/ROSA BUILDING BLOCK

| Number of building blocks (*N*) | 1 | 2 | 3 |
|---|---|---|---|
| Measured EVM (dB) *N* physical transmissions | -26.9 | -25.8 | -24.8. |
| Measured EVM (dB) *N* emulated transmissions | -27.2 | -26 | -24.6 |

As it can be seen from Tab. IV, the agreement between measured EVM after physical transmissions and measured EVM obtained with emulation seems to validate the emulation protocol for RoF bus testing, considering this limited number of cascaded blocks. The small difference between EVM for the physical and emulated transmissions in Tab. IV may come from the difficulty we have found to reproduce exactly the same building blocks based on TOSA/ROSA for the *N* physical transmissions, since we do not have any industrial facility. It can also be concluded from Tab. IV that building block based on TOSA/ROSA induces severe limitations on the transmitter EVM. Since the maximum allowed EVM for WLAN 54 Mbps transmitter is -25 dB (Tab. II), only two building blocks based on TOSA/ROSA can be cascaded in the RoF bus infrastructure, which is extremely low. This result is due to the low input 1-dB compression point for the TOSA/ROSA optical link (Tab. I and Section III.B), mainly coming from the non-linearity of the ROSA transimpedance amplifier, ROSA's being dedicated to receive baseband digital signals.

### C. *Experimental Results for the RoF bus based on VCSEL/PIN*

Since our building block based on TOSA/ROSA exhibit poor performance for transmission to a large number of ANs in the RoF bus, only VCSEL/PIN optical link has been considered to be tested with the emulation protocol for a large number of building blocks. Experimental results for RoF bus down-link are reported on Fig. 5 and show EVM of WLAN after transmission over *N* building blocks using the aforementioned emulation protocol, constellation diagrams for 64 QAM OFDM for *N*=1 (inset (a) on Fig. 5) and *N*=20 (inset (b) on Fig. 5) have also been reported. EVM is measured at the RF front-end output, without radio propagation, and it has been compared with theoretical EVM computed from (10). After transmission over 10 building blocks, it can be observed that measured EVM with the emulation protocol slightly exceeds EVM predicted by theory. This result may come from the cumulative quantization noise from successive analog to digital conversions (ADC) and digital to analog conversions (DAC) introduced by the emulation protocol. Experimental results show that a maximum of *N*=19 building blocks can be cascaded in the RoF bus down-link to respect EVM limit at the RF-front-end output (Tab. II).

Radio coverage for both down-link and up-link are reported on Fig. 6. Down-link radio coverage has been measured moving the WLAN receiver to reach $SNR_{req}$ defined by the IEEE 802.11g standard (Tab. II). It is found that the down-link radio coverage is around 4.5 m for a maximum number of building blocks of 18, for which the noise induced by the cascaded building blocks stay in the limit for acceptable EVM at the transmitter output. The coverage distance is smaller than the 11 m expected from the theoretical approach (Section III.C), which may be due to the simplified free space propagation model used to evaluate *PL* (12). After transmission over 19 building blocks, down-link coverage drops, due to the impact of the transmitter EVM on the received SNR. For the up-link, only fewer measurement results have been reported on Fig. 6, due to the more complex and time consuming protocol, emulation being realized several times for a given number *N* of building blocks, to find out the up-link radio coverage distance satisfying the required $SNR_{req}$ at the central station WLAN receiver (Tab. II). As expected, it can be seen on Fig. 6, that the up-link radio coverage is found to increase when decreasing *N*, up-link sensitivity (15) being improved when decreasing *N*. Indeed, $G_{RF\ UL}$ has been set to obtain equal radio coverage for down-link and up-link for the last AN of the RoF bus (*N*=20 in (17)). Radio coverage for bidirectional transmission is the minimum between down-link and up-link radio coverages, it has not been reported on Fig. 6 for the sake of clarity.

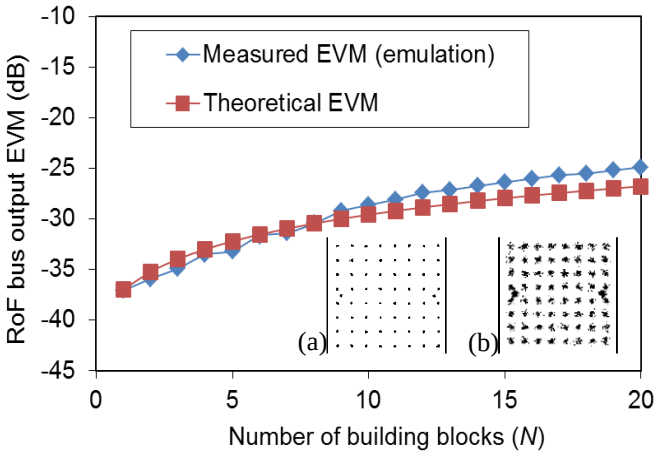


Figure 5. Measured EVM at access node output after emulated transmissions over *N* building blocks. Insets: Measured WLAN constellation diagram for *N*=1 (a), for *N*=20 (b).

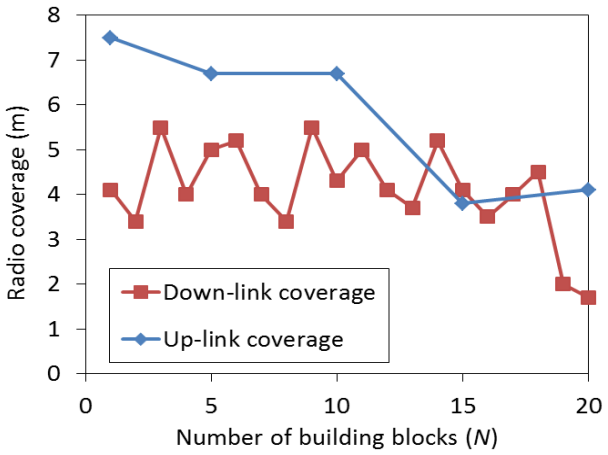


Figure 6. Measured downlink and up-link radio coverage with emulated transmissions over *N* building blocks.

## V. Discussion

### A. RoF star-bus for large building

It has been demonstrated in Section IV.C that RoF bus provides a bidirectional radio coverage of around 4.5 m per room for a data rate of 54 Mbps and for a maximum of *N*=18 rooms. However, for a large professional building, the number of rooms may exceed *N*=18. In that case, it is necessary to extend the concept of the proposed RoF bus topology to a RoF star-bus topology [4].

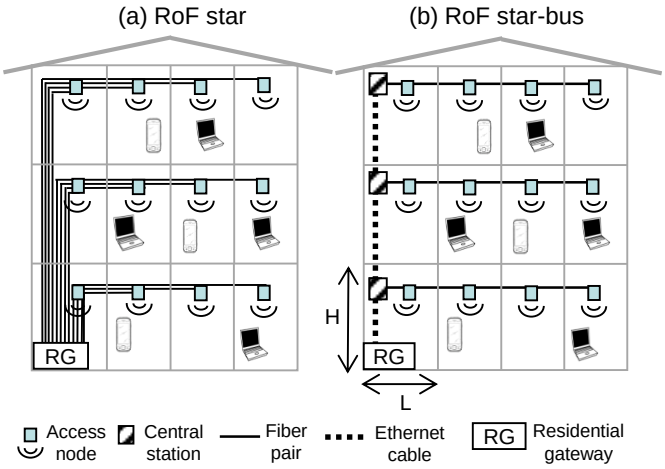


Figure 7. (a) RoF star, (b) RoF star-bus network topologies.

As shown in Fig. 7.b, the RoF star-bus topology would make it possible to attribute, for example, one or several RoF bus per floor, if the number of rooms per floor is smaller than 18. The RoF star-bus topology uses one central station per RoF bus. All central stations are also connected to the residential gateway using Ethernet connection available in the building as for connection of WLAN access points in classical radio deployment. RoF star-bus infrastructure would provide maximum data rate WLAN communications in each room of the building, using low emitted power closer to the user and ensuring a better control of the radiated power in the whole building. Several access node RF front-ends may be switched off in case no user is present in the room or confidentiality is required in a meeting room, as a consequence power consumption of the RoF bus would be decreased. Due to the low transmission power of the access nodes and of the WLAN mobile units (emitting power of -20.5 dBm vs 17 dBm for a typical WLAN transmitter), the maximum radiated optical field is drastically reduced inside the building [14] and battery powered mobile units (laptops, smartphones using WLAN connections) decrease their overall energy consumption and increase their autonomy.

### B. Comparison between RoF star and RoF star-bus in-building fiber length deployment

Fiber deployment cost is a significant part of the overall in-building optical network deployment [15], [23]. To make the comparison between the deployed fiber length required for RoF star network (Fig. 7a) and our proposed RoF star-bus infrastructure (Fig. 7.b), we consider a building with *M* floors, *N* rooms per floor, each room being with surface *L*x*L* and heigh *H*. All rooms are equipped with one AN, located in the center of the room ceiling. The fiber deployment for the RoF star infrastructure (Fig. 7.a) requires a fiber pair between the residential gateway and each access node so the overall fiber length ($L_{fiber\ star}$) to deploy is:

$$L_{fiber\ star} = M(M+1)H + MN^2L \qquad (18)$$

For the RoF star-bus infrastructure (Fig. 7.b), supposing one optical RoF bus to be deployed per floor and that Ethernet cable is already available inside the building to connect the bus central stations to the residential gateway, the overall fiber length ($L_{fiber\ star\text{-}bus}$) to deploy is defined as:

$$L_{fiber\ star-bus} = M(2N-1)L \qquad (19)$$

From (18) and (19), considering *M*=5, *N*=18, *H*=3 m and *L*=8 m, a 89% reduction of fiber length is obtained for the RoF star-bus compared to the RoF star topology.

### C. Connection to multiple access nodes

A mobile unit having the possibility to connect to multiple ANs, a RoF bus DAS has the potential to introduce significant delay spread. The magnitude of the delay spread can be significant in the RoF bus since ANs are fed with different fiber lengths. It has been shown in [13], for a star network infrastructure, that fiber length differences larger than 30 m introduce severe degradation on WLAN signal due to a significant increase of delay spread relatively to the OFDM guard interval duration, leading to OFDM intersymbol interferences.

Considering the aforementioned RoF bus deployment scenario considered in Section V.A (*N*=18, 2 neighbored ANs being separated by *L*=8 m) for one floor, the maximum fiber length difference introduced by the RoF bus between the first AN and the $N^{th}$ AN would be around 136 m which is above the 30 m limit. However, the radiated power in the proposed RoF bus DAS is extremely low, and we may expect that the reduced emitted power from any WLAN transmitter will be detected by the closest AN, and only by the first neighbored ANs, which would introduce delay spread from fiber length difference of

only 16 m. Additional investigations are under considerations to validate this hypothesis.

## VI. Conclusion

In this paper, a RoF bus DAS has been demonstrated for in-building wireless network, where one AN is deployed per room with a limited transmitted power and radio coverage. The novelty of the proposed RoF bus infrastructure is to use cascaded building blocks fulfilling the condition for gain transparency, using electronic coupling and in-line amplification in the AN, providing extended reach and low cost approach compared to a RoF bus based on optical power splitters.

Optical links of the cascaded building blocks exhibit non-linearity and a careful modulation power must be defined to minimize the impact of the reduced the 1-dB compression point for the overall RoF bus. RoF bus down-link and up-link noise figures are impacted by the cascade of building blocks. For the RoF bus up-link, an amplifier is required in the RF front-end to achieve equivalent radio coverage for down-link and up-link, providing bi-directional communications.

For the first time, a demonstration of the RoF bus is provided, considering two different optical links based on the use of low cost VCSEL/PIN or TOSA/ROSA optical links. Characterizations of the optical links have shown limited performance of the TOSA/ROSA solution compared to the VCSEL/PIN due to the poor linearity of our ROSA receiver. A specific experimental protocol, based on the use of signal emulation, has been especially defined to test the RoF bus for large number of ANs. Validation of the experimental approach has been successfully demonstrated, comparing the EVM results after physical transmission over 3 cascaded building blocks based on TOSA/ROSA, showing good agreement with experimental results using the emulation protocol. Nevertheless, since TOSA/ROSA based building block induces significant impact from our ROSA non-linearity, the transmission is limited to a maximum over 3 cascaded building blocks. It must be noticed here, that several ROSA's exhibiting higher linearity have been reported in literature [24], which implies that ROSA may still be considered as a valuable candidate for RoF bus technology, with the benefit of very low cost component, since ROSAs are massively produced for 10 Gbps Ethernet applications.

For a larger number of cascaded building blocks, the VCSEL/PIN optical link has been considered for the RoF bus demonstration. The experimental results from the emulation protocol have shown the possibility of transmitting the WLAN signal over 19 building blocks before achieving the maximum EVM allowed by the 802.11g standard for the WLAN transmitter. RF power for WLAN transmitters (ANs and mobile devices) is extremely reduced (-20.5 dBm) compared to the typical WLAN transmitter power (17 dBm) used in pure radio network, leading to a significant decrease of the maximum radiated power inside the building, and an increase of autonomy for battery powered mobile devices. LOS radio coverage distance has been measured to be around 4.5 m for bidirectional transmission at a maximum data rate of 54 Mbps, for a maximum of 18 ANs. The radio coverage distance is found to be lower than the expected radio coverage estimated by the theoretical approach, which may be attributed to the simplified free space path loss model considered in the theoretical approach.

Finally, for a large building DAS, a RoF star bus topology is proposed, based on the use of one RoF bus per building floor, interconnecting central stations with Ethernet cables to the residential gateway. With this topology, large buildings, with number of rooms larger than 18 can be equipped with the RoF bus technology, and the fiber length to be deployed in the building has been found to be 89% lower than for the a RoF star topology. Since fiber deployment in the building take a significant part in the overall cost of the fiber DAS network cost, the star bus topology may appear as a cost effective solution for in-building DAS.

## References


[1] L. G. Kazovsky, T. Ayhan, A. S. Gowda, A. R. Dhaini, A. Ng'oma, P. Vetter, "Green in-building networks: The future convergence of green, optical and wireless technologies," in *Transparent Optical Networks (ICTON), 2013 15th International Conference on*, pp. 1–5, 2013.

[2] G. Keiser, "Network implementation trade-offs in existing homes," *Ultra-Modern Telecommunications and Control Systems and Workshops (ICUMT), 2012 4th International Congress on*, pp. 528-532, 2012.

[3] A. Attar, H. Li, V. C. Leung, "Green last mile: how fiber-connected massively distributed antenna system can save energy," *IEEE Wireless Communications*, vol. 18, n°5, pp. 66-74, Oct. 2011.

[4] A. M. J. Koonen, H. P. A. van den Boom, H.-D. Jung, H. Yang, E. O. Martinez, P. Guignard, E. Tangdiongga, "Photonic in-building networks - architectures and advanced techniques," in *Proc. International Conf. on Optical Internet*, Jeju, South Korea, pp. 1–3, Aug. 2010,

[5] M. Sauer, A. Kobyakov, J. George, "Radio Over Fiber for Picocellular Network Architectures," *Journal of Lightwave Technology*, vol. 25, nº 11, p. 3301-3320, Nov. 2007.

[6] G. Gordon, M. Crisp, R. Penty, I. White, "Experimental Evaluation of Layout Designs for 3x3 MIMO-Enabled Radio-over-Fiber Distributed Antenna Systems," *IEEE Tans. Vehicular Technologies*, to be published, 2013.

[7] M. J. Crisp, S. Li, A. Wonfor, R. V. Penty, I. H. White, "Demonstration of radio over fibre distributed antenna network for combined in-building WLAN and 3G coverage," in *Optical Fiber Communication Conference*, conference proceedings, 2007.

[8] Y. Le Guennec, A. Pizzinat, S. Meyer, B. Charbonnier, P. Lombard, M. Lourdiane, B. Cabon, C. Algani, A.-L. Billabert, M. Terre, C. Rumelhard, J.-L. Polleux, H. Jacquinot, S. Bories, C. Sillans, "Low-Cost Transparent Radio-Over-Fiber System for In-Building Distribution of UWB Signals," *IEEE/OSA Journal of Lightwave Technoogy*, vol. 27, no. 14, pp.2649-2657, Jul. 2009.

[9] Y. Yang, C. Lim, A. Nirmalathas, "Digitized RF-over-fiber technique as an efficient solution for wideband wireless OFDM delivery," *Optical Fiber Communication Conference*, 2012, p. OTu2H–6.

[10] D. Wake, A. Nkansah, N. J. Gomes, "Radio Over Fiber Link Design for Next Generation Wireless Systems," *IEEE/OSA Journal of Lightwave Technology*, vol. 28, nº 16, p. 2456-2464, Aug. 2010.

[11] A. Das, A. Nkansah, N. J. Gomes, I. J. Garcia, J. C. Batchelor, D. Wake, "Design of low-cost multimode fiber fed indoor wireless networks," *IEEE Trans. Microw. Theory Tech.*, vol. 54, no. 8, pp. 3426–3432, Aug. 2006.

[12] A. Das, M. Mjeku, A. Nkansah, N. J. Gomes, "Effects on IEEE802.11 MAC throughput in wireless LAN over fibre systems," *IEEE/OSA Journal of Lightwave Technology*, vol. 25, pp. 3321-3328, Nov. 2007.

[13] M. J. Crisp, Sheng Li, A. Watts, R. V. Penty, I. H. White, "Uplink and Downlink Coverage Improvements of 802.11g Signals Using a Distributed Antenna Network," *IEEE/OSA Journal of Lightwave Technology*, vol. 25, nº 11, pp. 3388-3395, Nov. 2007.

[14] Y. Josse, B. Fracasso, et P. Pajusco, "Model for energy efficiency in radio over fiber distributed indoor antenna Wi-Fi network," *Wireless*

*Personal Multimedia Communications (WPMC), 2011 14th International Symposium on*, Brest, France, Oct. 2011.

[15] A. M. J. Koonen, H. P. A. van den Boom, E. O. Martinez, A. Pizzinat, P. Guignard, B. Lannoo, C. M. Okonkwo, E. Tangdiongga, "Cost optimization of optical in-building networks," *Optics Express*, vol. 19, nº 26, p. B399-B405, Nov. 2011.

[16] Y. Shi, C. M. Okonkwo, A. M. J. Koonen, E. Tangdiongga, "Large-core plastic optical fibre based in-home optical networks," in *Optical Network Design and Modeling (ONDM), 2012 16th International Conference on*, p. 1–5, 2012.

[17] Z. Bouhamri, Y. Le Guennec, J-M. Duchamp, G. Maury, Armin Schimpf, V. Dobremez, L. Bidaux, B. Cabon, "Multistandard RoF bus for in-building networks," *Microwave Photonics, 2011 IEEE International Topical Meeting on*, conference proceedings, Singapore, Oct. 2011.

[18] B. Razavi, "RF Microelectronics: International Edition," ed. Pearson, 2011.

[19] C. Lethien, C. Loyez, J.-P. Vilcot, R. Kassi, N. Rolland, C. Sion, P.-A. Rolland, "Review of glass and polymer multimode fibers used in a wimedia ultrawideband MB-OFDM radio over fiber system," *IEEE/OSA Journal of Lightwave Technology*, vol. 27, no. 10, pp. 1320–1331, May 2009.

[20] R. A. Shafik, S. Rahman, A. R. Islam, "On the extended relationships among EVM, BER and SNR as performance metrics," in *Electrical and Computer Engineering, 2006. ICECE'06. International Conference on*, pp. 408–411, 2006.

[21] A. F. Molisch, "Wireless Communications," ed. Wiley, 2010.

[22] Z. Bouhamri, Y. Le Guennec, J-M Duchamp, G. Maury, B. Cabon, "Quasi-static approach to optimize RF modulation of vertical-cavity surface-emitting lasers," *Microwave Photonics, 2011 IEEE International Topical Meeting on, conference proceedings*, Montréal, Canada, Oct. 2011.

[23] T. Koonen, H. Van den Boom, E. Tangdiongga, H.-D. Jung, P. Guignard, "Designing in-building optical fiber networks," in *National Fiber Optic Engineers Conference*, conference proceedings, San Diego, CA, Mar. 2010.

[24] J. Guillory, Y. Ait Yahia, A. Pizzinat, B. Charbonnier, C. Algani, M. D. Rosales, J. L. Polleux, "Comparison between two 60GHz multipoint RoF architectures for the Home Area Network," in *Networks and Optical Communications (NOC), 2012 17th European Conference on*, pp. 1–5, 2012.